CrossMark

Effect of substrate temperature and post-deposition annealing on intrinsic a-SiO$_x$:H film for n-Cz-Si wafer passivation

Yuping He[1,2] · Haibin Huang[1] · Lang Zhou[1] · Zhihao Yue[1] · Jiren Yuan[1]

Abstract In order to make sure the co-operation of substrate temperatures and post-deposition annealing on the structure and performance of the a-SiO$_x$:H for n-Cz-Si wafer passivation, three series a-SiO$_x$:H films bifacial-deposited on n-Cz-Si wafers were made. In which, the first series was deposited at room temperature and post-deposition annealing with different temperature; the second series was deposited with different substrate temperature and without post-annealing; and the third series was deposited with different substrate temperature and post-annealed at the optimized 275 °C. Effective lifetime of the samples was tested by QSSPC method, and the imaginary part of dielectric constant (ε_2) and film properties of the films were analyzed by Spectroscopic Ellipsometry and Fourier Transform Infrared Spectroscopy. It is concluded that (1) the structure and passivation effect of a-SiO$_x$:H films on n-Cz-Si wafer are sensitive to the substrate temperature and post-deposition annealing, and the optimum scheme is depositing the film at 100 °C and post-annealing the wafer at 275 °C; (2) the microstructure parameter R^* of the a-SiO$_x$:H is ~0.67 for the samples with the optimum passivation effect.

1 Introduction

The intrinsic passivation layers play a key role to reduce the surface state density of the silicon wafer and improve the photoelectric conversion efficiency of the crystalline silicon heterojunction solar cells [1]. It is one of core technologies behind the record conversion efficiency for HIT solar cell of Panasonic Corporation [2]. In which oxygen doped amorphous silicon (a-SiO$_x$:H) is a good choice for the material of the intrinsic thin-layer [1]. It is well known that the substrate temperature during the film deposition has great effect on the properties of the a-SiO$_x$:H films [3], and on the effect of the film on the c-Si wafer passivation [4]. Muller et al. [5] also showed that the low temperature (250 °C) post-annealing process has effect on the passivation of a-SiO$_x$:H film on c-Si wafer. For the mechanism of the temperature of the thermal processing affecting on the a-SiO$_x$:H passivating the c-Si wafer surface, there is no exact explanation. Jaran et al. [6] mentioned that the Si–(OH)$_x$, Si–O–Si bonds in the film have some effect to reduce the defects in the films and improve the passivation effect. It is thought that this is not exact enough to show the mechanism of the c-Si surface passivation by a-SiO$_x$:H, for the Si–H$_x$ bonds [7], crystalline quality [8] also changed during the thermal processing. In order to understand the performance and the mechanism more clearly, some series of samples with widely arranged temperatures for the as-deposition and post-annealing processes for the a-SiO$_x$:H films on c-Si wafer were designed. The samples were analyzed with Spectroscopic Ellipsometry (SE) and Fourier Transform Infrared Spectroscopy (FTIR), in order to understand the influence the temperature of deposition and post-deposition annealing have on the property and performance of the a-SiO$_x$:H films more unequivocal.

✉ Haibin Huang
haibinhuang@ncu.edu.cn

1 Institute of Photovoltaics, Nanchang University, Nanchang 330031, China

2 School of Science, Nanchang Institute of Technology, Nanchang 330099, China

Springer

2 Experimental

The silicon wafers used are n type Czochralski monocrystalline Si (100), with a thickness of 180 μm, resistivity of 3 Ω cm and a size of 40×40 mm^2. Before passivation layers deposition, the wafers were cleaned by acetone, then etched about 25 μm each side by KOH solution (20 wt%, 85 °C) for 20 min, then cleaned by SC1 solution (80 ml H_2O_2 + 80 ml NH_4OH + 400 ml H_2O, 80 °C) for 10 min and SC2 solution (80 ml H_2O_2 + 80 ml HCl + 400 ml H_2O, 80 °C) for 10 min, last dipped in HF solution (2 vol%) for 1 min to removing the native oxide layers.

The passivation layer is hydrogenated amorphous silicon sub-oxides (a-SiO$_x$:H) on both sides of the n-Cz-Si wafers by AC glow discharge of plasma (13.56 MHz, CCP type) enhanced chemical vapor deposition (PECVD, HW-PECVD-1E, Weina Ltd. China), and the source gases are silane (SiH$_4$), hydrogen (H$_2$) and carbon dioxide (CO$_2$). All the thicknesses of the deposited layers are about 100 nm. Gas flux ratios are SiH$_4$:H$_2$:CO$_2$ = 3:15:0.6 (sccm), air pressure is 22 Pa; power is 12 W, 10 min.

After deposition, some samples are post-annealed for 1 h by Halogen-lamp heating furnace, in argon atmosphere and under atmospheric pressure.

The lifetime of the samples before and after the post-annealed processes was tested by RF-PCD method, Sinton WCT-120. The hydrogen bonds structure of the passivation layers was tested by Fourier infrared spectrometer (FTIR, Nicolet 380). The imaginary dielectric factor of the wafers was analyzed by Spectroscopic Ellipsometry (Semilab, GES5-E).

3 Results and discussions

3.1 The influence of the post-deposition annealing temperature

The post-deposition annealing temperatures of each wafer are 200, 250, 275, 300, and 350 °C respectively. The effective lifetime of an as-deposited wafer and all the post-annealed wafers are shown in Fig. 1.

Figure 1 shows the results of effective lifetime of n-Cz-Si wafers passivated by a-SiO$_x$:H, with and without post-annealing. Figure 1a shows that passivation effect of a-SiO$_x$:H deposited at room temperature is poor. The post-deposition annealing has great effect on improving the passivation effect of the a-SiO$_x$:H layers as Fig. 1b, for the lifetime of the post-annealed wafer increases greatly. The maximum value of the lifetime of the wafers belongs to the wafer post-annealed at 275 °C, the value is

1371 μs (at a minority carrier density of 1×10^{15} cm^{-3}). For calculation of surface recombination velocity (SRV) S_{eff}, it is assumed that both surfaces provide a sufficiently low recombination velocity (less than D/4w [9, 10], D is the diffusion coefficient, about 35 cm^2/s, w is the thickness of wafer, about 180 μm), and have the same values $S_{eff} = S_{front} = S_{back}$, as the sample structure is symmetric. The surface recombination velocity can be deduced by Eq. (1) [5]:

$$S_{eff} = \left(\frac{1}{\tau_{eff}} - \frac{1}{\tau_{bulk}} \right) \times \frac{w}{2} \qquad (1)$$

In which w is the wafer thickness, τ_{bulk} is set infinity (an upper limit of the SRV is calculated for the case that no SRH recombination is considered by setting $\tau_{bulk} \to \infty$ in Eq. 1). From Eq. (1) S_{eff} of the wafer annealed at 275 °C is 4.7 cm/s. The results of imaginary part of dielectric constant (ε_2) and Raman spectra of samples are shown in Fig. 2.

Figure 2a shows ε_2 spectra of n-Cz-Si passivated by a-SiO$_x$:H at room temperature without and with annealing. The spectra of the samples with annealing temperature below 300 °C show peaks at about 3.6 eV, are typical of amorphous silicon characteristic spectrum [8, 11, 12]. The Raman results of Fig. 2b show that a-Si peak of the films covered wafers appear obviously around 480 cm^{-1} compare to that of the naked Si wafer, but the peak density of the Si–O–Si bond does not depend on a-SiO$_x$:H film. It is unambiguous that the films in this series are amorphous silicon structure without detectable SiO$_2$ structure [5, 10]. With the increasing of the thermal annealing temperature, ε_2 peak slightly shifts to higher energy, but significantly turns to lower energy when the temperature is higher than 300 °C. It can be explained that the SiH$_n$ stretching modes change in the films [13, 14], the FTIR spectra and microstructure parameter R^* of the samples are fitted by "multiple peak fit" function of Origin in Fig. 3. The R^* defined by Eq. (2) [15]

$$R^* = \frac{I_{2090}}{I_{2000} + I_{2090}} \qquad (2)$$

Figure 3 is SiH$_n$ of the samples with different post-deposition annealing temperatures and microstructure parameters R^*. The ratio of the fitted peaks area can be characterized with the relative content of SiH and SiH$_2$ bonds in the a-SiO$_x$:H films [2]. The peaks are at 2000 and 2090 cm^{-1} corresponds to SiH bond and SiH$_2$ bond, respectively. Because of oxygen attachment, the peak of SiH$_2$ shifts to a higher wave number [6]. Figure 3 can infer that the passivation effect is the best when R^* at an appropriate proportion.
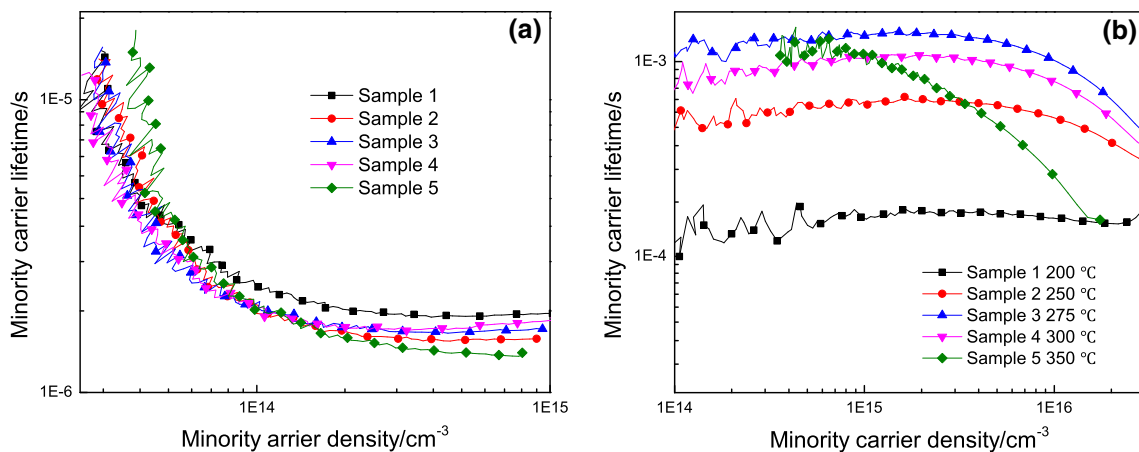
Fig. 1 The effective lifetime of n-Cz-Si wafers passivated by a-SiO$_x$:H. **a** As-deposited; **b** post-annealed at different temperatures
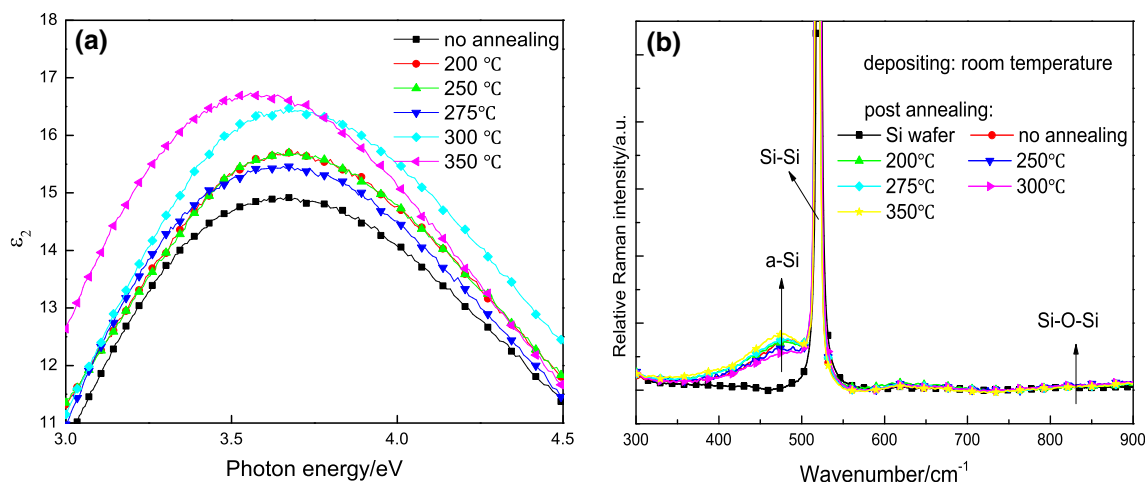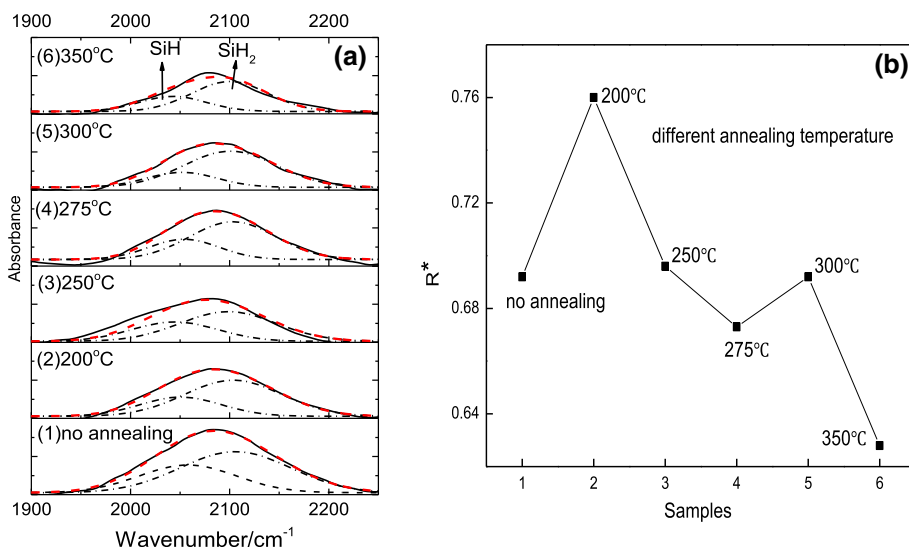

Fig. 2 **a** The ε_2 of the annealed wafers with different annealing temperature; **b** Raman spectra

Fig. 3 **a** SiH$_n$ of the samples with different post-annealing temperatures; **b** microstructure parameters R^*
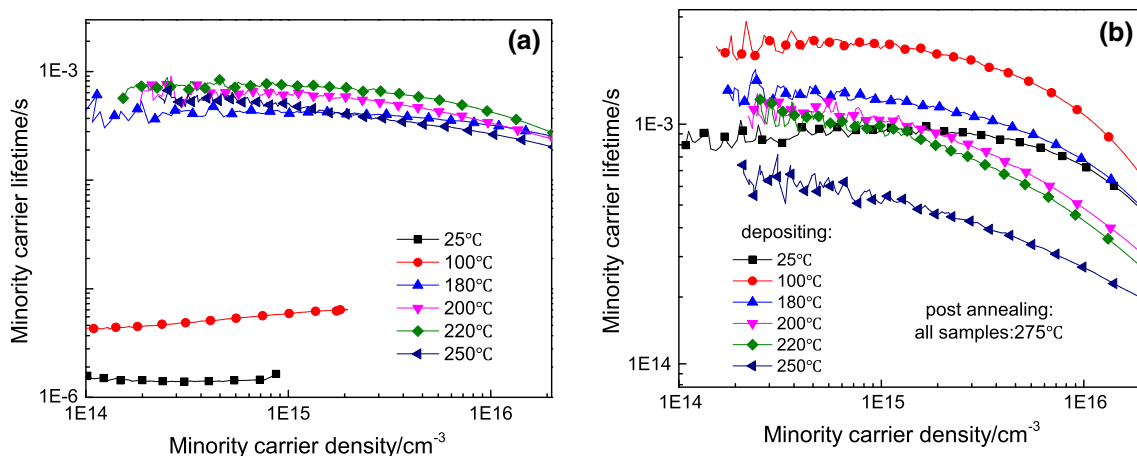
Fig. 4 **a** The lifetime of the same wafers with *a*-SiOₓ:H layers as-deposited at different substrate temperatures; **b** annealed at 275 °C
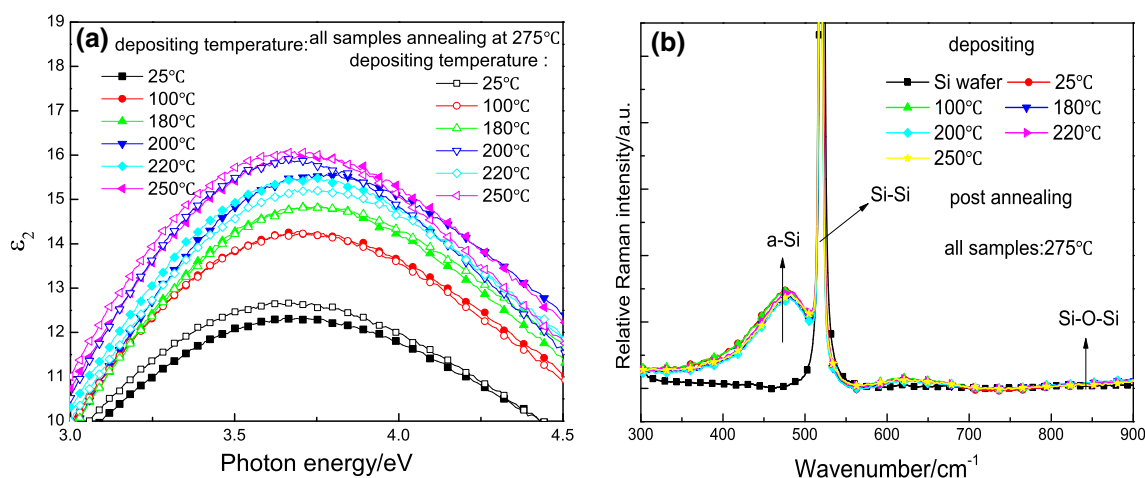

Fig. 5 **a** The ε_2 spectra of samples before and after the post-annealing process; **b** the Raman spectra of samples after post-annealing

3.2 The co-operation effect of the substrate-heating during the deposition process and the post-deposition annealing process

This series of samples is deposited at different substrate heating temperatures, and post-annealed at 275 °C for 1 h. The substrate heating temperature during film deposition are 25, 100, 180, 200, 220, and 250 °C, respectively. The tested effective lifetimes of the wafers as-deposited and post-annealed are shown in Fig. 4.

Figure 4 shows the effective lifetime of the post-annealed n-Cz-Si wafers with passivation layers at 275 °C. The insert shows the lifetime of the same wafers with *a*-SiOₓ:H layers as-deposited at different substrate temperatures. It is clear that with the substrate temperature increasing, the effective lifetime increases firstly and then decreases, the optimum passivation effect is gained at the substrate temperature of 220 °C with the highest lifetime of

747 μs (at a minority carrier density of 1×10^{15} cm^{-3}). The result is similar with the optimum temperature 210 °C in Ref. [9].The post annealing process at 275 °C has great effect on improving the effective lifetime of most of the samples significantly. The highest effective lifetime value is 2135 μs (at a minority carrier density of 1×10^{15} cm^{-3}) and belongs to the sample with the films deposited at 100 °C. Since the thickness of the wafer is 130 μm, the surface recombination velocity is 3.1 cm/s according to the Eq. (1), which is good enough for silicon heterojunction solar cells. The ε_2 and Raman spectra of samples are shown in Fig. 5.

Figure 5a is the ε_2 spectra of n-Cz-Si wafers before and after the post-annealing deposited *a*-SiOₓ:H films with different temperature. All the spectra show a broad peak at around 3.6 eV, which shows that thin films in the samples, are amorphous silicon structured [8, 16]. The hollow symbols in Fig. 6 represent the ε_2 spectra of wafers after

Fig. 6 a SiHn bonds of the samples with different deposition temperatures and the same post-annealing 275 °C; **b** microstructure parameters R*
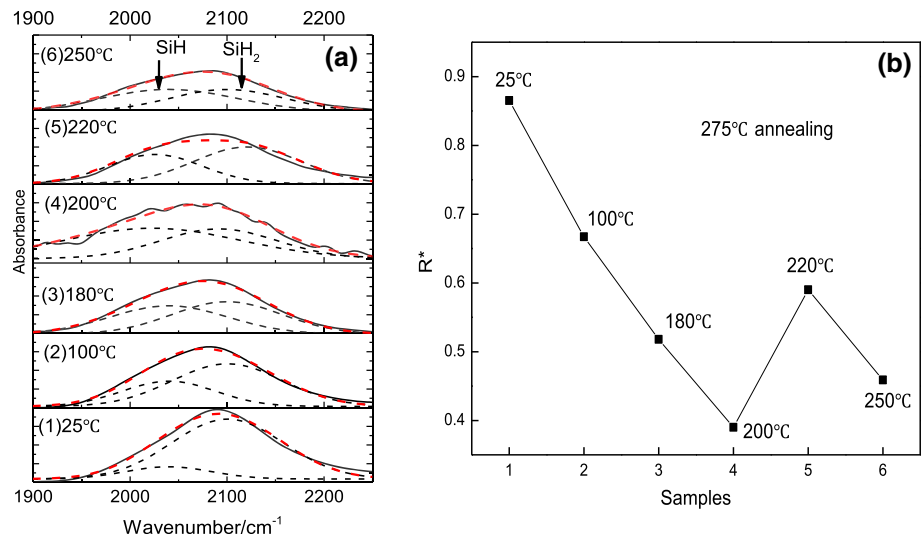
annealing with 275 °C. It is shown that the amplitude and peak position decrease with increasing post-annealing temperature, significantly for the samples of deposited temperature higher than 200 °C. It can be explained that with the increasing of temperature, these trends are consistent with hydrogen in the films reducing at higher temperatures [15]. From the Raman spectra of the samples shown in Fig. 5b, it can be further clarified that the films on the samples are mainly amorphous silicon structure. The SiH_n microstructure and its parameter R^* of samples are shown in Fig. 6.

Figure 6 indicate that SiH_n bonds composition and microstructure parameter R* change with deposition temperature increasing, although the samples underwent the same post-annealing process. According to Figs. 3 and 6, passivation effect is optimum when R^* is about 0.67, the performance of a-SiO$_x$:H films is highly sensitive to the content of H and SiH_n bonds composition [13, 17], the H content and SiH_n bonds composition of a-SiO$_x$:H film is closely affected by the thermal processes, both deposition and post-annealing.

4 Conclusions

In order to understand the effect of temperature of the deposition and post-annealing processes on intrinsic a-SiO$_x$:H film for n-Cz-Si wafer passivation, three series samples with different film deposition temperature or/and different post-annealing temperature are prepared and analyzed. It can be concluded that: (1) the structure and passivation effect of a-SiO$_x$:H films on n-Cz-Si wafer are sensitive to the temperature of the deposition and post-annealing processes, the optimum scheme is depositing at 100 °C and post-annealing at 275 °C; (2) the microstructure

parameter $R^*$of the a-SiO$_x$:H is $\sim$0.67 for the samples with the optimum passivation effect.

References

1. H. Haibin, Z. Donghua, W. Yilin et al., Optimization and operation mechanism analysis of Cz-Si wafer passivation by a-SiOx:H film. J. Func. Mater. **9**(45), 07001–07004 (2014)
2. K. Wakisaka, M. Taguchi, T. Sawada et al., More than 16% solar cells with a new "HIT" (doped a-Si/non doped a-Si/crystalline Si) structure. in *Proceedings of the 22nd IEEE Photovoltaic Specialists Conference*, Las Vegas, NV, USA, pp. 887–892 (1991)
3. J.A. Luna-López, G. García-Salgado, T. Díaz-Becerril et al., FTIR, AFM and PL properties of thin SiOx films deposited by HFCVD. Mater. Sci. Eng., B **174**, 88–92 (2000)
4. T.H. Wang, E. Iwaniczko, M.R. Page et al., Effect of emitter deposition temperature on surface passivation in hot-wire chemical vapor deposited silicon heterojunction solar cells. Thin Solid Films **501**, 284–287 (2006)
5. T. Mueller, S. Schwertheim, W.R. Fahrner, Crystalline silicon surface passivation by high-frequency plasma-enhanced chemical vapor-deposited nanocomposite silicon suboxides for solar cell applications. J. Appl. Phys. **107**, 014504 (2010)
6. J. Sritharathikhun, C. Banerjee, M. Otsubo et al., Surface passivation of crystalline and polycrystalline silicon using hydrogenated amorphous silicon oxide film. Jpn. J. Appl. Phys. **6A**(46), 3296–3300 (2007)
7. S.R. Jadkar, J.V. Sali, S.T. Kshirsagar, Influence of process pressure on HW-CVD deposited a-Si: H films. Sol. Energy Mater. Sol. Cells **85**, 301–312 (2005)
8. A.F. Morral, P.R. Cabarrocas, Structure and hydrogen content of polymorphous silicon thin films studied by spectroscopic ellipsometry and nuclear measurements. Phys. Rev. B **69**, 125307 (2004)

9. A.B. Sproul, Dimensionless solution of the equation describing the effect of surface recombination of carrier decay in semiconductors. J. Appl. Phys. **76**, 2851–2854 (1994)

10. J. Brody, A. Rohatgi, A. Ristow, Review and comparison of equations relating bulk lifetime and surface recombination velocity to effective lifetime measured under flash lamp illumination. Sol. Energy Mater. Sol. Cells **77**, 293–301 (2003)

11. T. Mueller, S. Schwertheim, W.R. Fahmer. Application of wideband gap hydrogenated amorphous silicon oxide layers to heterojunction solar cells for high quality passivation. IEEE, (2008). doi:10.1109/PVSC.2008.4922792

12. D. Levi, E. Iwaniczko, M. Page et al., Silicon heterojunction solar cell characterization and optimization using in situ and ex situ spectroscopic ellipsometry, in *IEEE*, Hawaii (2006). doi:10.1109/WCPEC.2006.279828

13. T. Mueller, J. Wong, A.G. Aberle, Heterojunction silicon wafer solar cells using amorphous silicon suboxides for interface passivation. Energy Proced. **15**, 97–106 (2012)

14. D.H. Levi, C.W. Teplin, E. Iwaniczko et al., Real-time spectroscopic ellipsometry studies of the growth of amorphous and epitaxial silicon for photovoltaic applications. J. Vac. Sci. Technol. **24**(4), 1676–1683 (2006)

15. J.D. Ouwens, R. Schrop, Hydrogen microstructure in hydrogenated amorphous silicon. Phys. Rev. B **54**(24), 17759 (1996)

16. I. Roca, P. Cabarrocas, C. Clerc, I. Fontcuberta, A. Morral, Structure and hydrogen content of polymorphous silicon thin films studied by spectroscopic ellipsometry and nuclear measurements. Phys. Rev. B **69**(12), 125307 (2004)

17. J.-C. Hsiao, C.-H. Chen, C.-C. Lin et al., Effect of hydrogen dilution on the intrinsic *a*-Si: H film of the heterojunction silicon-based solar cell. J. Electrochem. Soc. **158**(9), H876–H878 (2011)